© 2015. Published by The Company of Biologists Ltd | Journal of Cell Science (2015) 128, 888–899 doi:10.1242/jcs.155499

RESEARCH ARTICLE

TRPP2-dependent Ca^{2+} signaling in dorso-lateral mesoderm is required for kidney field establishment in *Xenopus*

Mélinée Futel[1,2], Catherine Leclerc[3,4,*], Ronan Le Bouffant[1,2], Isabelle Buisson[1,2], Isabelle Néant[3,4], Muriel Umbhauer[1,2], Marc Moreau[3,4] and Jean-François Riou[1,2,*]

ABSTRACT

In *Xenopus laevis* embryos, kidney field specification is dependent on retinoic acid (RA) and coincides with a dramatic increase of Ca^{2+} transients, but the role of Ca^{2+} signaling in the kidney field is unknown. Here, we identify TRPP2, a member of the transient receptor potential (TRP) superfamily of channel proteins encoded by the *pkd2* gene, as a central component of Ca^{2+} signaling in the kidney field. TRPP2 is strongly expressed at the plasma membrane where it might regulate extracellular Ca^{2+} entry. Knockdown of *pkd2* in the kidney field results in the downregulation of *pax8*, but not of other kidney field genes (*lhx1*, *osr1* and *osr2*). We further show that inhibition of Ca^{2+} signaling with an inducible Ca^{2+} chelator also causes downregulation of *pax8*, and that *pkd2* knockdown results in a severe inhibition of Ca^{2+} transients in kidney field explants. Finally, we show that disruption of RA results both in an inhibition of intracellular Ca^{2+} signaling and of TRPP2 incorporation into the plasma membrane of kidney field cells. We propose that TRPP2-dependent Ca^{2+} signaling is a key component of *pax8* regulation in the kidney field downstream of RA-mediated non-transcriptional control of TRPP2.

KEY WORDS: Pronephros, Ca^{2+} signaling, TRPP2, Pax8, *Xenopus*

INTRODUCTION

The vertebrate kidney originates from the dorso-lateral mesoderm and develops through the formation of three successive renal structures; the pro-, meso- and meta-nephros. These three structures represent organs of increasing complexity, which contain a similar basic unit of filtration, the nephron. The structure of the nephron and the molecular mechanisms involved in its formation are evolutionarily conserved (Dressler, 2009; Saxen, 1987; Vize et al., 2003). In *Xenopus laevis* tadpoles, the functional pronephros is made of a single nephron, thus providing a simple system to study how pluripotent mesodermal cells are committed to a renal fate (Jones, 2005).

Specification of mesodermal cells to a pronephric fate is achieved at late gastrula and early neurula stages. Dorso-lateral mesodermal explants isolated at these stages differentiate into the glomus and tubule (Brennan et al., 1998; Brennan et al., 1999). Several genes encoding transcription factors whose murine orthologs are known to play an important function during renal development (Dressler, 2009) are expressed in this territory at the onset of neurulation. They include *pax8*, *lhx1*, *osr1* and *osr2* (Carroll and Vize, 1999; Tena et al., 2007). Loss of function of *osr1*, *osr2* (Tena et al., 2007) and *lhx1* (Chan et al., 2000) impair the development of the pronephros, whereas overexpression of *pax8* and/or *lhx1* results in the development of ectopic and enlarged pronephroi (Carroll and Vize, 1999). The mesodermal territory where *pax8* and *lhx1* expression overlap has been defined as the pronephric field or kidney field.

The mechanisms controlling kidney field emergence from the mesodermal layer at gastrula stages are only partially understood. Retinoic acid (RA) signals during gastrulation are absolutely required. Disruption of RA signaling results in a loss of *pax8* and *lhx1* expression in the kidney field, and in a loss of glomus and tubule development at later stages (Cartry et al., 2006). Wnt-11b induces pronephric structures in unspecified lateral mesoderm explants, and also acts as a potential inducer (Tételin and Jones, 2010). In contrast, FGF signaling needs to be downregulated to allow mesodermal cells to adopt a pronephric fate (Colas et al., 2008; Le Bouffant et al., 2012).

Ca^{2+} signaling is also an important regulator of pronephric tubule differentiation. Previously we have recorded transient increases in intracellular Ca^{2+} concentrations ($[Ca^{2+}]_i$) in the dorso-lateral mesoderm with maximum of Ca^{2+} activities at early neurula stage, that is, coinciding with kidney field specification. The spatial distribution of Ca^{2+} transients in cultured kidney field explants are concentrated within the area where the pronephric tubule will later differentiate. Inhibition of these transients with Ca^{2+} chelators at late gastrula or mid-neurula stages results in a defective development of the tubule (Leclerc et al., 2008). The origin of these Ca^{2+} transients has not been attributed to specific channels. However, the inhibitory effect of lanthanum chloride (La^{3+}), a potent antagonist of most transient receptor potential (TRP) channels (Clapham et al., 2005), on tubulogenesis strongly suggests that TRP channels are involved in the process (Leclerc et al., 2008). One likely candidate is TRPP2.

TRPP2 (also known as polycystin-2 and encoded by the *pkd2* gene), is a member of the TRP superfamily of channels, which are known to function as non-selective cation channels that are permeable to Ca^{2+} (Köttgen, 2007). TRPP2 can function at several subcellular locations, including the basolateral plasma membrane of epithelial cells (Ma et al., 2005), endoplasmic reticulum (ER), where it might operate as a Ca^{2+}-release channel (Koulen et al., 2002) and primary cilia, where it is thought to participate in mechanosensation (Nauli et al., 2003). At primary cilia, the function of TRPP2 has been linked to kidney cysts formation in

[1]Université Pierre et Marie Curie-Paris VI, Equipe 'Signalisation et Morphogenèse', UMR7622-Biologie du Développement, 9, quai Saint-Bernard, 75005 Paris, France. [2]CNRS, Equipe 'Signalisation et Morphogenèse', UMR7622-Biologie du Développement, 9, quai Saint-Bernard, 75005 Paris, France. [3]Université Toulouse 3, Centre de Biologie du Développement, 118 route de Narbonne, F31062 Toulouse, Cedex 04, France. [4]CNRS UMR5547, Toulouse F31062, France.

*Authors for correspondence (jean-francois.riou@upmc.fr; catherine.leclerc@univ-tlse3.fr)

Received 18 April 2014; Accepted 5 January 2015

Journal of Cell Science

Journal of Cell Science (2015) 128, 888–899 doi:10.1242/jcs.155499

vertebrates. Human *PKD2* mutations are responsible for a large number of cases of autosomal dominant polycystic kidney disease (ADPKD) (Mochizuki et al., 1996) and null mutation of the murine ortholog *Pkd2* is embryonic lethal. *Pkd2* mutants exhibit severe cardio-vascular defects, and form cysts in developing nephrons and pancreatic duct (Wu et al., 2000). Morpholino-based loss of function of *pkd2* also results in the formation of pronephric cysts during zebrafish development (Obara et al., 2006; Sun et al., 2004) and in the formation of severe edema and of dilated pronephric tubules in *Xenopus* (Tran et al., 2010).

Here, we address the potential role of TRPP2-dependent Ca^{2+} signaling during early pronephros development in *Xenopus* embryos and show that TRPP2 is involved in the formation of the kidney field. *Pkd2* loss of function causes a severe inhibition of *pax8* expression in the kidney field. Interestingly, expression of other kidney field genes such as *osr1*, *osr2* and *lhx1* is unaffected. Furthermore, morpholino (MO)-mediated *pkd2* depletion results in a dramatic decrease of the number of Ca^{2+} transients in kidney field explants, showing that TRPP2 is directly involved in the generation of Ca^{2+} signaling in this region of the embryo. Using a photo-inducible Ca^{2+} chelator, we show that kidney field expression of *pax8* is decreased when Ca^{2+} signaling is inhibited from the midgastrula stage. This function of TRPP2 is associated with the localization of TRPP2 to the plasma membrane and not to the primary cilium. We further show that both Ca^{2+} signaling and TRPP2 incorporation into the plasma membrane are both dependent on RA signaling, suggesting that RA might play an important function in the control of Ca^{2+} signaling in the kidney field. Taken together, these data provide evidence that TRPP2-dependent Ca^{2+} signaling is acting very early during development to specifically control the expression of *pax8*, a master gene regulator of pronephric kidney development.

RESULTS

TRPP2 expression peaks at the late gastrula stage when the $[Ca^{2+}]_i$ increase reaches its maximum in the emerging kidney field

Our previous data suggest that Ca^{2+} signaling during pronephros induction *ex vivo* by activin and RA involves TRP family channels (Leclerc et al., 2008). Therefore, to determine whether TRPP2 might be required during kidney field formation *in vivo*, we analyzed its expression during development using a cross-reacting antibody directed against human TRPP2 (supplementary material Fig. S1). TRPP2 expression was analyzed by western immunoblotting on whole embryo extracts. TRPP2 was detected throughout development (Fig. 1A). Although TRPP2 was only barely detected during segmentation stages and early gastrulation, expression levels raised at midgastrula stage [Nieuwkoop and Faber (NF) stage 11] to reach a maximum at the end of gastrulation. TRPP2 expression then dropped during neurula and early tailbud stages (NF stage 14–22), and increased again from mid-tailbud stage (NF stage 25) onwards, to reach high levels in the early tadpole (NF stage 35/36). The first period of high TRPP2 expression at the late gastrula stage therefore coincides with the maximum increase of $[Ca^{2+}]_i$ in the kidney field of whole embryos (Leclerc et al., 2008). It is also interesting to note that the second period of high TRPP2 expression is correlated with tubule differentiation, where TRPP2 is known to play an important function (Tran et al., 2010).

We have further studied the localization of TRPP2 in cells of kidney field explants isolated at the late gastrula stage (NF stage 13), using immunofluorescence staining and confocal microscopy. In explants isolated from embryos expressing membrane-targeted GFP, anti-TRPP2 immunoreactivity colocalized with GFP, suggesting that TRPP2 is expressed at the plasma membrane (Fig. 1B).

TRPP2 has been found to be located to primary cilia in mammalian cells (Pazour et al., 2002; Yoder et al., 2002). In *Xenopus* neurula, TRPP2 is expressed in cilia of the gastrocoel roof plate (GRP), a ciliated epithelium forming the dorsal surface of the archenteron. TRPP2 in GRP plays a crucial role in the establishment of left–right asymmetry (Schweickert et al., 2007). At the tailbud stage, TRPP2 is also associated with cilia in another epithelium, the pronephric nephron tubule (Tran et al., 2010). We tested for the presence of cilia in cells from kidney field explants isolated at early (NF stage 13–14) or late (NF stage 18) neurula stage using anti-acetylated tubulin antibodies (supplementary material Fig. S2). GRP and kidney field are

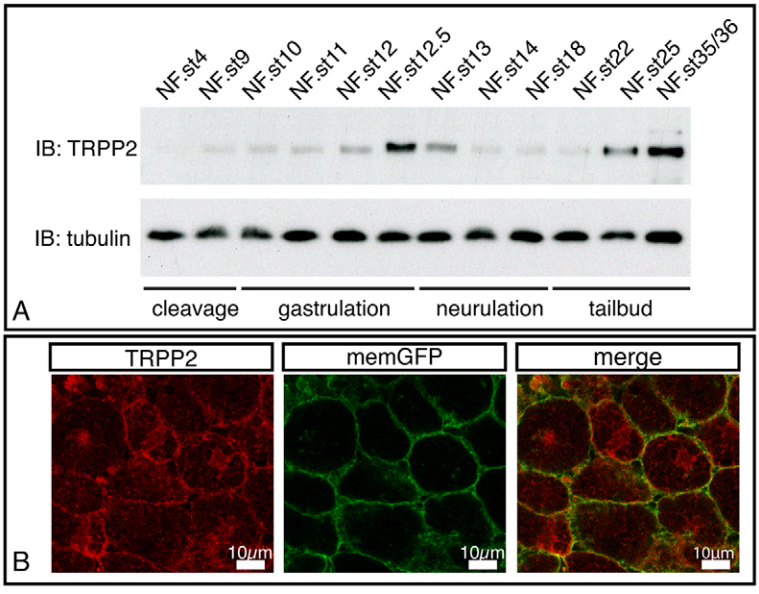

Fig. 1. TRPP2 is expressed in the kidney field. (A) Temporal analysis of TRPP2 expression during development. TRPP2 is detected by immunoblotting throughout development but its expression increases during gastrulation (NF stage 10 to stage 13) to reach a maximum at the late gastrula stage (NF stage 12.5). Expression then diminishes to increase again at late tailbud and early tadpole stages (from NF stage 25 onwards).
(B) Immunolocalization of TRPP2 in kidney field cells. Expression of plasma-membrane-targeted GFP (memGFP) was carried out by mRNA microinjection at the four-cell stage. Double immunostaining for TRPP2 and GFP. Immunoreactivity for the anti-TRPP2 antibody colocalizes with GFP, indicating that TRPP2 is expressed at the plasma membrane. Scale bars: 10 μm.

Journal of Cell Science (2015) 128, 888–899 doi:10.1242/jcs.155499

different embryonic tissues. As a positive control for the presence of cilia, GRP explants were taken at the same stages. No cilia-like structures were observed in kidney field explants, whereas they were readily detected in the GRP. In order to further attempt to detect cilia, we expressed an mCherry-tagged version of the axoneme protein arl13b (Borovina et al., 2010; Caspary et al., 2007; Chung et al., 2012), and analyzed its distribution in kidney field and GRP cells at NF stage 14. mCherry–arl13b was clearly localized in GRP cilia but never in kidney field cells (supplementary material Fig. S2). Our data strongly suggests that the function of TRPP2 at this early stage of kidney development is not linked to the primary cilium.

pkd2 knockdown results in the downregulation of *pax8* in the kidney field without affecting other kidney field genes

To determine whether TRPP2 is required for kidney field specification, we analyzed whether *pkd2* knockdown affects *pax8* expression using previously validated *pkd2*-specific translation-blocking antisense MOs (Pkd2-MO) (Tran et al., 2010). Pkd2-MO was injected at the four-cell stage into the two left blastomeres (2 pmoles per blastomere) in order to target the presumptive dorso-lateral mesoderm containing kidney field precursors on the left side of the embryo. The right side of the embryo provided an internal control. Embryos were then cultured until early neurula stage (NF stage 14–15) for *in situ* hybridization (ISH) analysis of *pax8* expression. Comparison of the left injected side and the right control side showed that *pkd2* knockdown resulted in a strong inhibition of *pax8* expression. Phenotypes ranged from a total extinction to a slight decrease of *pax8* expression (Fig. 2A). With Pkd2-MO alone, the strongest phenotypes (total extinction plus strong *pax8* inhibition) represented 91% of analyzed embryos ($n=91$). Control morpholino (CMO) injection (2 pmoles per blastomere) had no effect upon *pax8* expression ($n=37$) (Fig. 2A). In order to assess *pkd2* knockdown specificity, we tested whether co-injection of a Pkd2-MO-resistant version of *Xenopus pkd2* mRNA (1 ng) was able to rescue *pax8* expression. Co-injection of *pkd2* mRNA indeed resulted in a strong decrease of the strongest phenotypes (62%, $n=98$), and an increase of normal patterns of *pax8* expression in the kidney field (Fig. 2A). The difference observed between frequency of strongest phenotypes in Pkd2-MO injected embryos, and in Pkd2-MO plus *pkd2* mRNA-injected embryos is significant ($P<0.01$, Pearson's chi-square test of independence), showing that *pkd2* knockdown specifically causes *pax8* downregulation.

The induction of the kidney field has been proposed to depend on signals emanating from the paraxial mesoderm (Seufert et al., 1999; Tételin and Jones, 2010). In order to rule out the possibility that *pkd2* knockdown indirectly interferes with *pax8* expression in the kidney field by affecting paraxial mesoderm, we analyzed *myod* expression in *pkd2* morphant embryos. Pkd2-MO was injected at the four-cell stage into the two left blastomeres (2 pmoles per blastomere), and *pax8* and *myod* expression were investigated at early neurula stage (NF stage 14–15). Although *pax8* was readily downregulated on the injected side ($n=18/20$), the Pkd2-MO did not affect *myod* expression ($n=34/37$). Analysis of *mlc* expression in somitic mesoderm in later morphant tailbud stage embryos (NF stage 28) further confirmed that Pkd2-MO did not affect development of the somites ($n=17/17$) (supplementary material Fig. S3)

To study whether *pkd2* knockdown affects kidney field formation in a general manner, or whether it principally impacts upon *pax8*, we compared expression levels of *pax8*, *osr1*, *osr2* and *lhx1* in kidney field explants isolated from CMO- or Pkd2-MO-injected embryos. Explants were isolated at NF stage 13, and were further cultured until early (NF stage 14) or late (NF stage 18) neurula stages for quantitative real-time PCR (RT-QPCR) analysis. As expected from ISH data on whole embryos, *pkd2* knockdown resulted in a dramatic reduction of *pax8* expression at NF stage 14 (Fig. 2B). At NF stage 18, Pkd2-MO still caused a substantial inhibition of *pax8* expression, but this was less pronounced than that at NF stage 14 (supplementary material Fig. S4). In contrast, *pkd2* knockdown did not affect *osr1*, *osr2* or *lhx1* expression at NF stage 14. At NF stage 18 *pkd2* knockdown might cause a slight increase of *lhx1* expression, but *osr1* and *osr2* remain unaffected (Fig. 2B).

This shows that *pkd2* loss of function specifically targets *pax8* expression in the kidney field.

Disruption of intracellular Ca^{2+} signaling during gastrulation results in *pax8* inhibition in the kidney field

Intracellular Ca^{2+} increases are required for pronephric tubule differentiation *ex vivo* and in intact *Xenopus laevis* embryos (Leclerc et al., 2008). Inhibition of Ca^{2+} signaling with a photo-inducible Ca^{2+} chelator targeted to the kidney field results in defective pronephros tubulogenesis. This effect is observed either when the chelator is uncaged at late gastrula stage (NF stage 11–12.5), that is, prior to kidney field specification, or at neurula stage (NF stage 16–17) when the kidney field is already specified (Leclerc et al., 2008). However, it remains unclear whether the disruption of Ca^{2+} signaling affects *pax8* expression in the emerging kidney field (Carroll and Vize, 1999). To test this hypothesis, we injected the photo-inducible Ca^{2+} buffer diazo-2 (Adams et al., 1989) into the left V2 blastomere at the eight-cell stage in order to target the presumptive dorso-lateral mesoderm containing kidney field precursors on the left side of the embryo. The right side of the embryo provided an internal control. Injected embryos were cultured until NF stage 11, at which time diazo-2 was uncaged, and were then further cultured until early neurula stage (NF stage 14) for ISH analysis of *pax8* expression (Fig. 3A). Comparison of control and injected sides revealed a clear inhibition of *pax8* expression in the kidney field on the left side injected with diazo-2. Expression was totally abolished in 52% of cases ($n=17/33$), and strongly reduced in 33% of cases ($n=11/33$) (Fig. 3B). These observations show that disruption of Ca^{2+} signaling not only affects tubulogenesis at later stages of pronephric development (Leclerc et al., 2008), but also early *pax8* expression in the kidney field. Given that diazo-2 and *pkd2* knockdown both cause a similar inhibition of *pax8* expression, we also tested whether *pkd2* knockdown could affect tubulogenesis at later stages. Embryos injected with Pkd2-MO in the two left blastomeres as above (2 pmole per blastomere) were cultured until NF stage 39-40 to analyze proximal tubule differentiation using the 3G8 antibody, which marks the proximal pronephric tubule, the nephrostomes and otic vesicle (Vize et al., 1995). Comparison of 3G8 immunoreactivity on the control and injected sides clearly showed that tubulogenesis was impaired in all examined embryos ($n=14$) (Fig. 3C). These data show that disruption of Ca^{2+} signaling and *pkd2* knockdown produce very similar effects, and further argue for a role of Ca^{2+} signaling in controlling *pax8* expression during kidney field formation at neurula stage.

Pkd2 knockdown results in an inhibition of Ca^{2+} signals in kidney field explants at neurula stage

To determine whether the Ca^{2+} signals observed in the kidney field at neurula stage (Leclerc et al., 2008) require functional

Journal of Cell Science (2015) 128, 888–899 doi:10.1242/jcs.155499

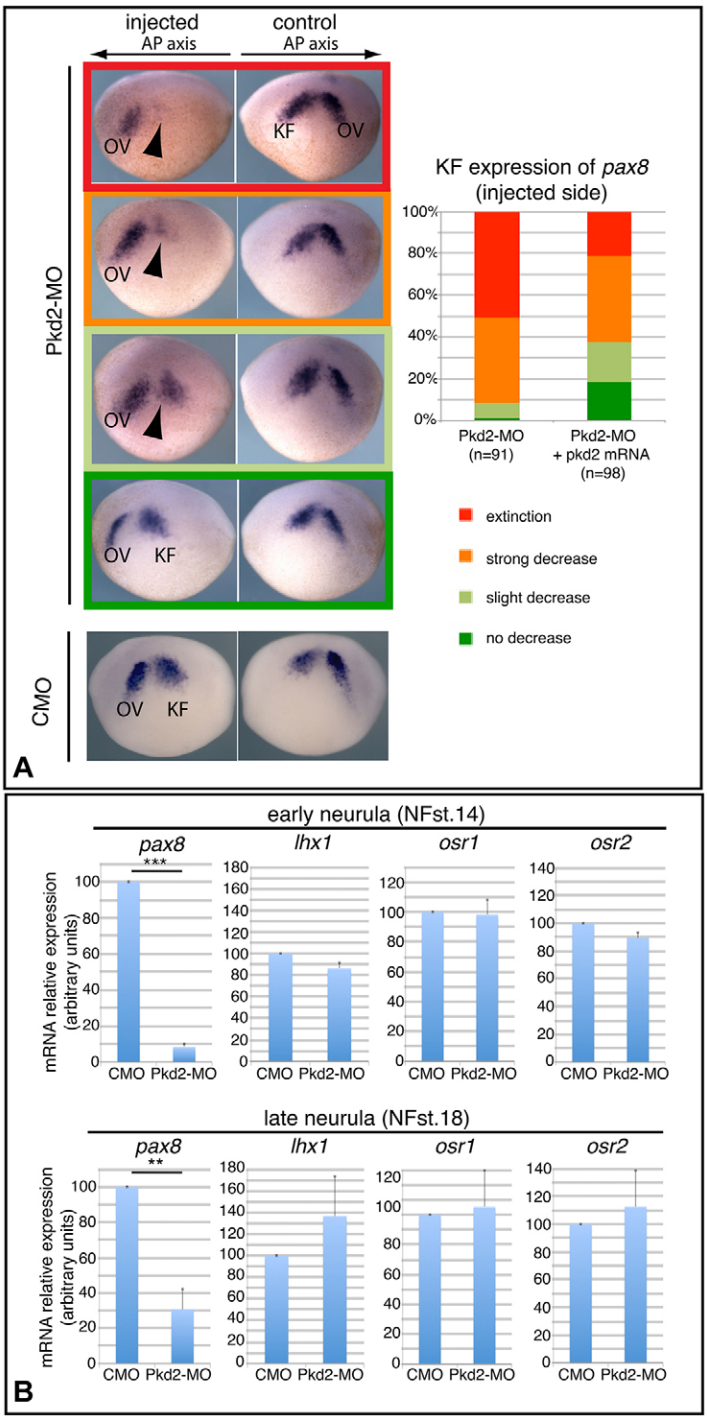

Fig. 2. *Pkd2* loss of function affects *pax8* expression in the kidney field. (A) *In situ* hybridization analysis of *pax8* expression in *pkd2* morphant embryos. Pkd2-MO was injected into the two left blastomeres at the four-cell stage and *pax8* expression was analyzed at early neurula stage (NF stage 14–15). Comparison of the left injected side with the right control side shows a strong inhibition of *pax8* expression in the kidney field (arrowheads). Extinction, or a strong decrease of *pax8* expression, is observed in more than 91% of the embryos analyzed. *Pax8* expression in CMO-injected embryos is unaffected. When a *pkd2* mRNA lacking the Pkd2-MO target sequence is co-injected with Pkd2-MO, this proportion is reduced to 62%, showing that it results to the specific loss of function of *pkd2*. OV, ectodermal expression of *pax8* in the presumptive otic vesicle; KF, mesodermal expression of *pax8* in the kidney field. Arrows indicate orientation of the antero-posterior (AP) axis. (B) RT-QPCR analysis of kidney field gene expression in dissected explants. CMO or Pkd2-MO was injected at the two-cell stage and embryos were cultured until late gastrula stage (NF stage 13) for kidney field explant dissection. Explants were further cultured until early neurula (NF stage 14) or late neurula (NF stage 18) stages for RT-QPCR analysis of *pax8*, *lhx1*, *osr1* and *osr2* expression. Mean±s.e.m. results from three independent experiments are displayed. As expected from the above results performed on whole embryos, there is a dramatic downregulation of *pax8* at the early neurula stage. In contrast, *lhx1*, *osr1* and *osr2* expression is not affected. At the late neurula stage, *pax8* expression is severely inhibited. In contrast, *lhx1*, *osr1* and *osr2* expression is not affected, indicating that Ca^{2+} signaling is acting upstream of *pax8*, but does not act in a general mechanism of kidney field induction. $^{**}P<0.01$, $^{***}P<0.001$ (paired Student's *t*-test).

TRPP2 Ca^{2+}-conducting channels, we depleted *pkd2*. Ca^{2+} recordings were performed using the bioluminescent Ca^{2+} reporter aequorin (Shimomura, 1991). Embryos were co-injected at the eight-cell stage into the V2 blastomere to target the kidney field with mRNA encoding aequorin fused to GFP, and Pkd2-MO (2 pmoles) (Tran et al., 2010) or CMO (2 pmoles). Embryos properly expressing GFP–aequorin in the kidney field were selected for dissection and Ca^{2+} recording at NF stage 12.5 (Fig. 4A). $[Ca^{2+}]_i$ measurements were carried out as previously described (Leclerc et al., 2008) for a period of 4 h, during which sibling controls evolved from the late gastrula (NF stage 12.5–13) to late neurula stage (NF stage 16–17). Recording of pairs of CMO and Pkd2-MO-expressing explants were always performed simultaneously.

Comparison of pairs of recordings always revealed a dramatic reduction of Ca^{2+} transients in kidney field explants expressing Pkd2-MO. Fig. 4B shows representative photo-multiplier tube (PMT) traces ($n=4$) obtained from pairs of kidney field explants dissected from CMO and Pkd2-MO injected embryos. A series of Ca^{2+} transients that appeared as vertical spikes on the time scale used, are observed on CMO kidney field data (Fig. 4B). The onset of Ca^{2+} transients occurred within 1 h after the beginning of

Journal of Cell Science (2015) 128, 888–899 doi:10.1242/jcs.155499

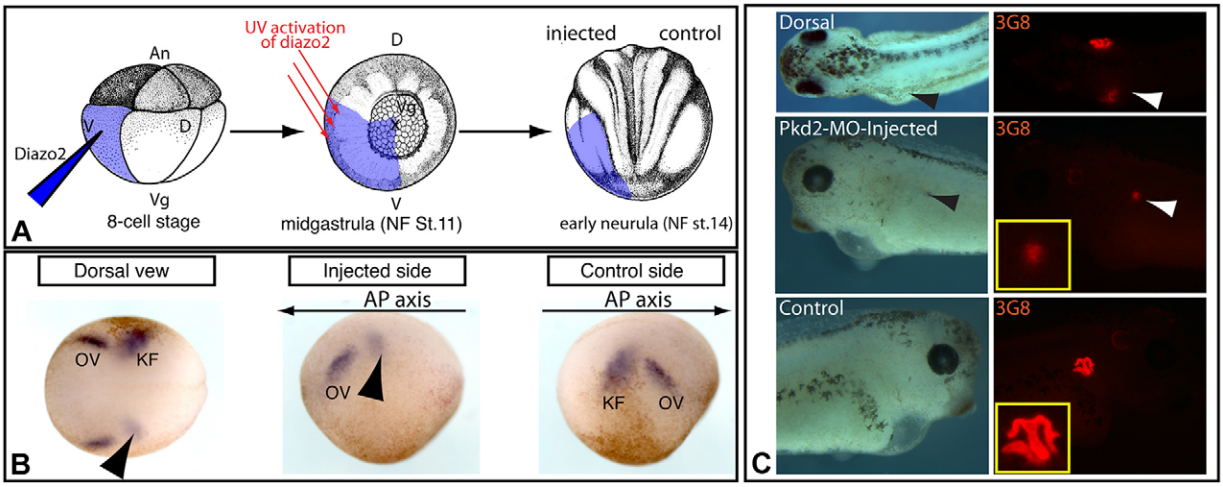

Fig. 3. Disruption of intracellular Ca^{2+} signaling results in the downregulation of *pax8* in the kidney field. (A) Schematic illustrating the experiment. Diazo-2 was injected at the eight-cell stage into the left V2 blastomere. Photoactivation of diazo-2 was performed at NF stage 11, and *pax8* expression was analyzed at the early neurula stage (NF stage 14). (B) Ca^{2+} chelation causes a downregulation of *pax8* in the kidney field (arrowheads). OV, ectodermal expression of *pax8* in the presumptive otic vesicle; KF, mesodermal expression of *pax8* in the kidney field. Arrows indicate orientation of antero-posterior (AP) axis. (C) Pkd2-MO causes impaired tubulogenesis at later stages. Pkd2-MO was injected into the two left blastomeres at the four-cell stage and 3G8 staining of pronephric tubules was carried out at NF stage 39–40. Pkd2-MO causes a severe reduction of the 3G8-positive tubule on the injected side (arrowheads).

the experiment, which corresponds to NF stage 13.5, when the kidney field is already specified. The maximum Ca^{2+} transient activity was reached at ~3 h, at about NF stage 15. The Ca^{2+} dynamics recorded from such kidney field explants were very similar to those observed previously (Leclerc et al., 2008). Interestingly, Ca^{2+} dynamics recorded from the Pkd2-MO kidney field were inhibited (Fig. 4B). The Ca^{2+} recordings were further analyzed by calculating the number, duration and the luminescence ratio (L/L_0) of the Ca^{2+} transients from four pairs of recordings over time for CMO and Pkd2-MO kidney fields (supplementary material Table S1). A histogram (Fig. 4C) shows that *pkd2* loss of function results in the significant reduction ($P=0.014$, paired Student's *t*-test) in the number of the Ca^{2+} transients without affecting the luminescence ratio of the transients (supplementary material Table S1). In order to control the specificity of Pkd2-MO effect, we attempted to rescue Pkd2-MO-inhibited Ca^{2+} signals by co-injecting an mRNA encoding a Pkd2-MO-resistant form of *pkd2* mRNA. Comparison of pairs of recording indicated that injection of the mutated form of *pkd2* mRNA (1 ng) was able to partially restore Ca^{2+} transients in kidney field explants (Fig. 4D, $n=3$). The average number of Ca^{2+} transients increased from 419 ($n=3$ explants) in explants expressing Pkd2-MO alone to 874 ($n=3$ explants) in explants expressing Pkd2-MO and *pkd2* mRNA (Fig. 4C; supplementary material Table S2). Although this increase is not statistically significant, a careful examination of the Ca^{2+} transients parameters revealed a significant increase in the duration of these Ca^{2+} transients (supplementary material Table S2; paired Student's *t*-test of three experiments, $P=0.016$) indicating that the overall Ca^{2+} level is higher in the explants expressing Pkd2-MO and *pkd2* mRNA. Taken together, these results show that *pkd2* knockdown results in an inhibition of Ca^{2+} signals in kidney field explants. This confirms that TRPP2 is involved in the generation of these signals.

In a further attempt to address the question of a direct role of TRPP2-dependent Ca^{2+} signaling in the regulation of *pax8* in the kidney field, we studied the possibility of rescuing *pax8* expression in Pkd2-MO morphants by artificially increasing intracellular Ca^{2+} with ionomycin. Embryos injected with Pkd2-MO in the two left blastomeres (1.6 pmole per blastomere) were cultured until late gastrula stage, at which stage beads soaked in ionomycin solution or in DMSO (controls), were implanted into dorso-lateral mesoderm, and embryos were further cultured for analysis of *pax8* expression. Beads can stay where they have been implanted for about 3 h by which time embryos have reached neurula stage (NF stage 14-15). Upon longer times of culture, we observed that beads are either expelled out of the embryo or fall into the archenteron, probably because of constraints resulting from neural tube closure. When *pax8* expression was analyzed 3 h after ionomycin bead implantation, no rescue could be observed. However, when cultured until late neurula stage (NF stage 19), a significant increase of *pax8* expression was observed in the ionomycin-soaked bead series relatively to the control bead series (supplementary material Fig. S4). This shows that increasing intracellular Ca^{2+} with ionomycin in the kidney field cells at early neurula stage can rescue, at least partly, *pax8* expression.

Disruption of RA signaling results in a strong decrease of kidney field intracellular Ca^{2+} signaling

Given that RA triggers an increase in $[Ca^{2+}]_i$ during pronephric tubule differentiation *in vitro* (Leclerc et al., 2008), we wanted to test whether RA is also important for the generation of Ca^{2+} transients during pronephros formation in the kidney field. To test this, Ca^{2+} transients were recorded in kidney field overexpressing the RA-catabolizing enzyme Cyp26. Embryos were either injected into the V2 blastomere with GFP–aequorin mRNA (control) or were co-injected with GFP–aequorin and Cyp26 mRNA (Cyp26) (350 pg). Ca^{2+} recordings were performed as previously on pairs of kidney field from NF stage 12.5 embryos. Disruption of RA signaling leads to the inhibition of Ca^{2+} signals as shown by the representative PMT traces for a pair of control and Cyp26 kidney field explants (Fig. 5A, $n=3$) and by the histogram plot of the average number of Ca^{2+} transients

Journal of Cell Science (2015) 128, 888–899 doi:10.1242/jcs.155499

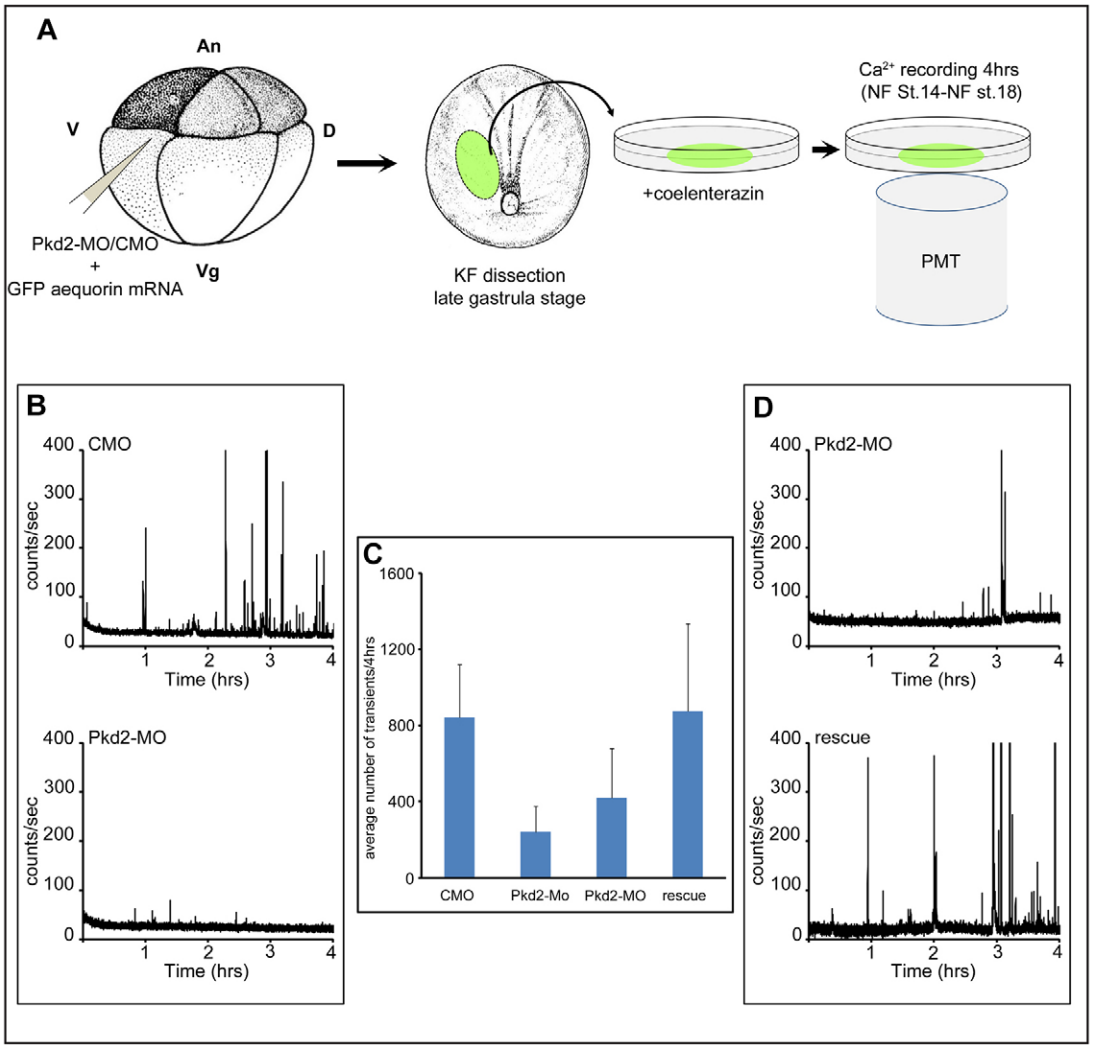

Fig. 4. A. Intracellular Ca^{2+} signaling in the kidney field requires TRPP2. (A) Schematic illustrating the procedure for Ca^{2+} measurements in the kidney field. CMO or Pkd2-MO morpholinos were injected in the V2 blastomere of eight-cell stage embryos along with GFP–aequorin mRNA. Kidney field (KF) explants were dissected at the late gastrula stage (NF stage 12.5) and Ca^{2+} transients were measured with a PMT for 4 h, until sibling developing embryos reach NF stage 18 (late neurula). (B) PMT traces from single pronephric territories dissected from control morpholino-injected embryo (CMO) and TRPP2 morpholino-injected embryo (Pkd2-MO). Data is representative of pairs of territories measured simultaneously in four independent experiments. (C) Histogram plot displaying the mean±s.e.m. number of Ca^{2+} transients during 4 h. The two left bars correspond to the mean±s.e.m. number of transients calculated for pairs of CMO and Pkd2-MO explants respectively (n=4 pairs). In this condition, Pkd2 knockdown significantly reduces the number of Ca^{2+} transients (P=0.014, paired Student's t-test). The two right bar plots correspond to pairs of Pkd2-MO and rescue (Pkd2-MO + pkd2 mRNA) explants, respectively (n=3 pairs). Although the number of Ca^{2+} transients increases in the rescue condition, it is not significant (see results for details). (D) Rescue of Ca^{2+} transients by *pkd2* expression in Pkd2-MO explants. Pkd2-MO and GFP–aequorin mRNA were injected alone or mixed with *pkd2* mRNA. PMT traces from single pronephric territories dissected from Pkd2-MO-injected embryo (Pkd2-MO) and embryo co-injected with Pkd2-MO and a Pkd2-MO resistant form of *pkd2* mRNA are shown. Data is representative of pairs of territories measured simultaneously from three independent experiments.

(Fig. 5B). The difference observed between the average number of Ca^{2+} transients in control- and Cyp26-mRNA-injected kidney fields is significant (P=0.008, paired Student's t-test of three pairs of experiments). These results raised the question of how RA is acting.

Therefore, we first tested the possibility that RA induces Ca^{2+} transients in the kidney field through the regulation of *pkd2* expression by analyzing whether RA signals disruption affects *pkd2* expression in lateral mesoderm explants. Expression of Cyp26 was targeted to the mesoderm by equatorial mRNA injection at the four-cell stage. Lateral marginal zone (LMZ) explants were dissected at early gastrula stage (NF stage 10), and cultured until early neurula stage (NF stage 14) for RT-QPCR analysis of *pkd2* expression (Le Bouffant et al., 2012). Although RA disruption readily causes *pax8* and *lhx1* downregulation, expression of *pkd2* was not affected (Fig. 6A). This shows that RA is not affecting TRPP2-dependent Ca^{2+} signaling in lateral mesoderm through the transcriptional regulation of *pkd2*.

Disruption of RA signaling causes a strong reduction in the amount of TRPP2 channel at the plasma membrane

We next asked whether RA signaling induces Ca^{2+} transients in the kidney field by regulating TRPP2 incorporation into the plasma membrane. To test this, we used total internal reflection fluorescence (TIRF) microscopy to visualize GFP-tagged TRPP2 proteins that are exclusively localized at the plasma membrane or

Journal of Cell Science (2015) 128, 888–899 doi:10.1242/jcs.155499

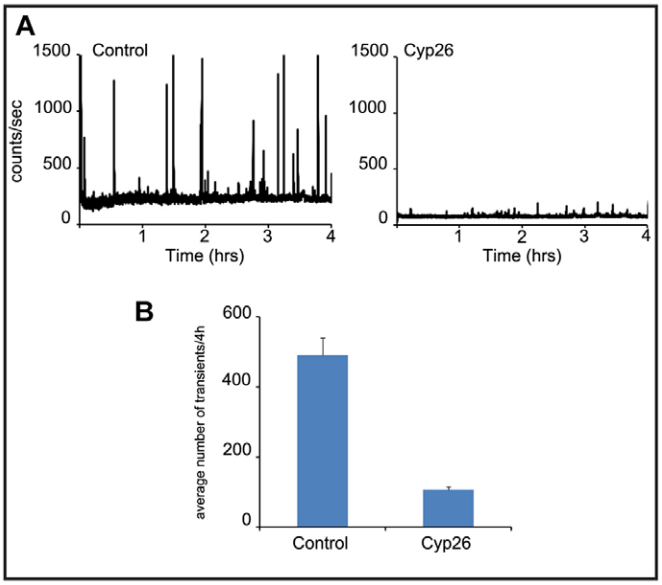

Fig. 5. Disruption of RA signaling inhibits intracellular Ca^{2+} signaling in the kidney field. (A) PMT traces from single pronephric territories dissected from control embryos injected with GFP–aequorin mRNA (Control) and embryos injected with GFP-æquorin mRNA plus Cyp26 mRNA (Cyp26). Representative data of pairs of territories measured simultaneously from three independent experiments. (B) Mean±s.e.m. number of Ca^{2+} transients during 4 h in control and Cyp26 conditions calculated for three independent pairs of experiments. Disruption of RA signaling significantly reduces the number of Ca^{2+} transients (P=0.008, paired Student's t-test).

in the 120 nm close to the membrane (Fig. 6A). mRNA coding a human GFP-tagged TRPP2 (hTRPP2–GFP) was injected into the V2 blastomere either alone (control) or in presence of Cyp26 mRNA to reduce RA signaling. Kidney field explants comprising ectoderm and mesoderm, and expressing hTRPP2–GFP were dissected at the end of gastrulation (stage 12.5–13), and the surface of mesodermal cells was analyzed by TIRF microscopy (Fig. 6B). The area of fluorescent spots per field in the presence and absence of Cyp26 mRNA (Fig. 6C) gives the proportion of TRPP2 channels localized close to the membrane. In the control condition, the calculated area of GFP spots was 220 µm^2 (n=51, four independent experiments). This area is reduced to 94.9 µm^2 (n=71, four independent experiments) in presence of 350 pg of Cyp26 mRNA (Fig. 6D), these results are in accordance with the reduction of Ca^{2+} signals observed in Fig. 5. The effect of RA disruption on the TRPP2 relocation is dose dependent; the co-injection of a 700 pg of Cyp26 mRNA results in a greater reduction in the area of GFP spots (28.9 µm^2, n=64, four independent experiments). These results show that RA signaling is affecting the incorporation of TRPP2 channels into the plasma membrane.

DISCUSSION

Several important conclusions can be drawn from this study. First, TRPP2 is expressed in the kidney field during specification and is not associated with cilia structures. Second, we report for the first time that *pkd2* loss of function is affecting early steps of *Xenopus* kidney development, that is, the establishment of the kidney field. Third, our data show that the Ca^{2+} transients observed in the kidney field during late gastrula and early neurula stages are due to the activation of TRPP2 channels. Furthermore, they strongly suggest that *pax8* expression is regulated by Ca^{2+} through a TRPP2-dependent mechanism acting upstream of the activation and/or maintenance of *pax8* expression in the kidney field. Fourth, we show that *pkd2* knockdown in the kidney field specifically affects *pax8* expression, but not *lhx1*, *osr1* and *osr2*, which implies that intracellular Ca^{2+} signaling is an intermediate step between the general mechanisms controlling kidney field emergence within latero-dorsal mesoderm and the control of *pax8* expression. Finally, we show that both intracellular Ca^{2+} signaling and incorporation of TRPP2 in the plasma membrane are both impaired upon disruption of RA signaling, suggesting that RA might control intracellular Ca^{2+} signaling in the kidney field.

Is TRPP2-dependent Ca^{2+} signaling control of *pax8* in renal precursors a specific feature of early *Xenopus* pronephros development?

Although several features of *pkd2* loss-of-function phenotypes are conserved among vertebrates, such as cystic kidneys and laterality defects, others already appear to be restricted to a species, as for example body curvature in zebrafish (Obara et al., 2006). Here, we report for the first time that *pkd2* loss of function affects early steps of *Xenopus* kidney development, that is, the emergence and/or the maintenance of the kidney field. This differs significantly from kidney *pkd2* loss-of-function phenotypes described in mouse (McGrath et al., 2003; Wu et al., 2000) or zebrafish (Bisgrove et al., 2005; Obara et al., 2006; Schottenfeld et al., 2007; Sun et al., 2004), where early kidney development does not appear to be affected. However, during mouse pronephric development it is unclear whether *Pkd2* does not have any function. Like in *Xenopus*, the commitment of mouse intermediate mesoderm to a kidney fate involves *Lhx1*, *Osr1*, *Osr2*, *Pax2* and *Pax8* (Dressler, 2009). Therefore, it is possible that, in the mouse, the pronephric development is impaired, but that further mesonephric development proceeds normally. Indeed, it has been shown, for example, that mouse pronephric development is severely compromised in *Raldh2*$^{-/-}$ embryos, but that *Pax2*-expressing prospective mesonephric collumns still develop (Cartry et al., 2006). In zebrafish, pan-embryonic and localized intercellular Ca^{2+} waves do affect the embryo during gastrulation. They are intense in the dorsal region of the embryo, but whether they have any function during kidney specification is unknown (Webb and Miller, 2006). Kidney specification in zebrafish might involve mechanisms differing from those underlying this process in *Xenopus*. It is noteworthy that RA disruption does not affect early kidney development in zebrafish as it does in *Xenopus* (Cartry et al., 2006; Wingert et al., 2007). Moreover, the consequence of *pkd2* loss-of-function upon *pax8* expression has not been investigated in zebrafish. Differences between zebrafish and *Xenopus* might also be the consequences of the respective roles played by the two closely related *pax* genes, *pax2* (*pax2a* in zebrafish) and *pax8*. In *Xenopus* only *pax8* is expressed in renal precursors of the kidney field, whereas both genes are expressed during early pronephric development in zebrafish (Majumdar et al., 2000). If TRPP2-dependent Ca^{2+} signaling is also acting upstream of *pax8* in zebrafish, *pkd2* loss-of-function would not cause early renal defects because of the redundancy between *pax2a* and *pax8*.

Ca^{2+} and other inputs regulating *pax8* in the kidney field

Our results show that Ca^{2+} signaling is required for the proper emergence and/or maintenance of the kidney field. It is likely that

Journal of Cell Science (2015) 128, 888–899 doi:10.1242/jcs.155499

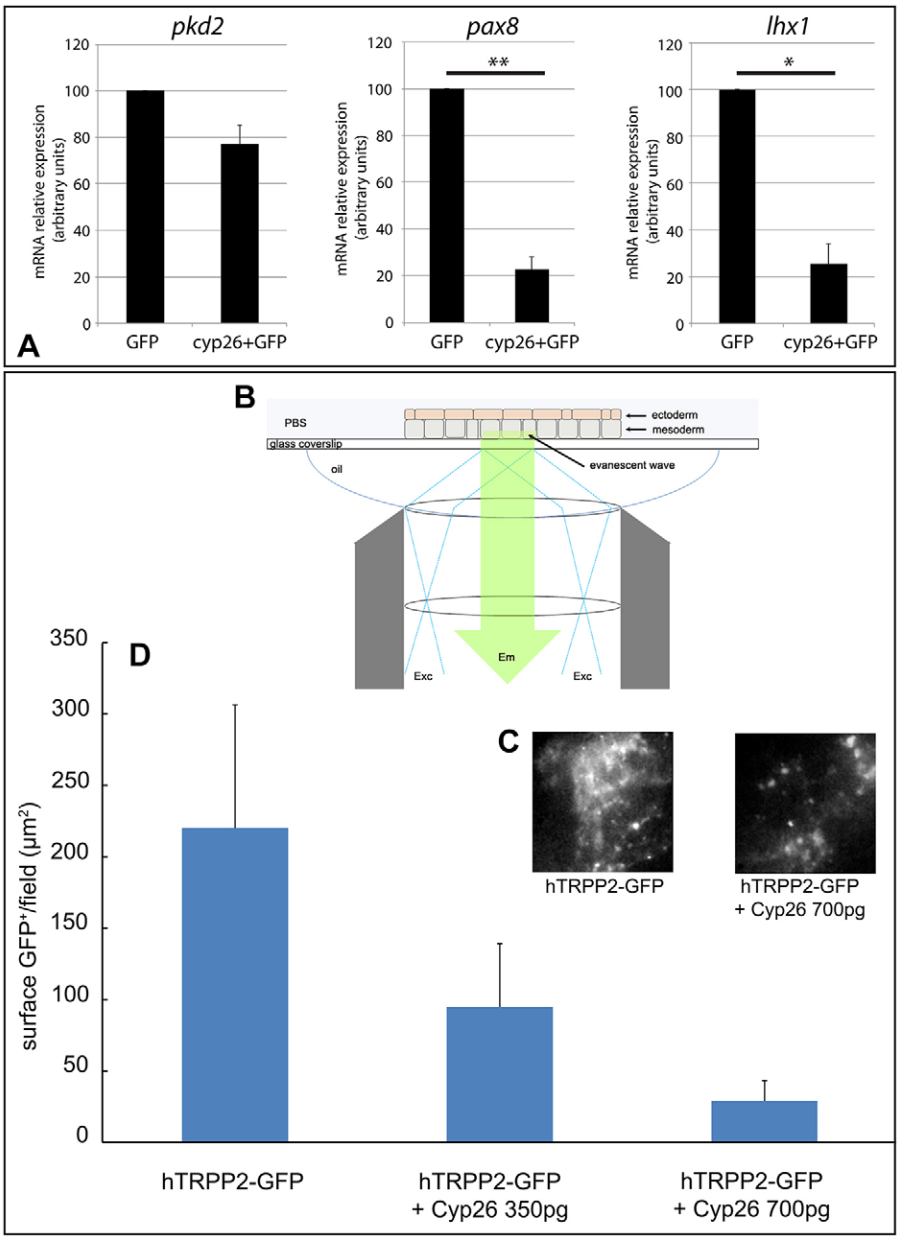

Fig. 6. Disruption of RA signaling relocates TRPP2 away from the plasma membrane. (A) RA disruption in lateral mesoderm does not affect *pkd2* expression. Isolated LMZ explants were taken from embryos previously injected with GFP mRNA (control) or with a mix of GFP and Cyp26 mRNA, and cultured until siblings reached the early neurula stage (NF stage 14) for RT-QPCR analysis. Mean±s.e.m. results from three independent experiments are shown. Although disruption of RA signaling causes a strong inhibition of *pax8* and *lhx1* expression, *pkd2* expression is not significantly affected. $*P<0.05$; $**P<0.01$ (paired Student's *t*-test) (B) Schematic representation of TIRF microscopy. TIRF microscopy exclusively images signals arising close to the cell membrane. TIRF works by directing excitation light through a glass substrate towards an aqueous specimen at an angle to obtain total internal reflection due to the refractive index decrease at the glass–water interface. In these conditions, an evanescent wave is created in the liquid with the same wavelength as the incident light. This evanescent wave decreases exponentially with distance. The wave is able to excite fluorophores only near the interface. It provides an 'optical sectioning' effect similar to, but even narrower, than that achieved by a confocal microscope (Axelrod, 2008). (C) Representative views of the imaging field for a hTRPP2–GFP mRNA-injected explant (left) and for an explant co-injected with hTRPP2–GFP mRNA and Cyp26 mRNA (right). (D) Histogram (mean±s.e.m.) displaying the calculated area of GFP spots per field of view (50×50 µm) in control kidney fields (hTRPP2–GFP) and in kidney fields overexpressing the RA-catabolizing enzyme Cyp26. 350 and 700 pg of Cyp26 mRNA was injected. Disruption of RA signaling induces the relocation of TRPP2 proteins away from the plasma membrane. This effect is dose-dependent.

Ca^{2+}-signaling-dependent regulation of *pax8* takes place downstream of the signals potentially responsible for kidney field specification during gastrulation, such as RA (Cartry et al., 2006) or Wnt11b (Tételin and Jones, 2010). In this work we show that a TRPP2-dependent Ca^{2+} signaling is not acting upstream of *lhx1*, *osr1* or *osr2*. It is thus possible that some of these genes might be regulated more directly by the kidney field specification signals than *pax8*. For example, *lhx1* upregulation in response to exogenous RA at the neurula stage occurs within 20 min, and is observed in the absence of protein synthesis, suggesting a direct regulation, whereas *pax8* upregulation is only observed after 2 h, suggesting an indirect response to RA (Cartry et al., 2006). In addition, kidney field expression of *pax8* is also likely to be dependent on other inputs, such as those mediated by bone morphogenetic proteins (BMPs), whose disruption during neurulation results in a loss of *pax8* expression (Bracken et al., 2008). Although we are not addressing the mechanisms by which Ca^{2+} controls *pax8* expression, an interesting possibility would be that the $[Ca^{2+}]_i$ increase acts as a release of *pax8* transcriptional repression. Regulation of *Pax8* during murine thyroid cell differentiation has indeed been shown to be dependent on a Ca^{2+}-dependent release of repression involving the Ca^{2+}-binding protein downstream response element-antagonist modulator (DREAM, also known as calsenilin, KCHIP3 or KCNIP3) (D'Andrea et al., 2005).

How might kidney field inductive signals act upon intracellular Ca^{2+} signaling?

How the $[Ca^{2+}]_i$ increase is related to more general mechanisms of kidney field induction remains elusive. Activation of non-canonical pathways by Wnt11b might act as a potential mechanism triggering the increase of $[Ca^{2+}]_i$ in the kidney field. Some Wnts are acting through the activation of phospholipase C and inositol 1,4,5-trisphosphate (IP_3) production. IP_3 in turn activates Ca^{2+} release from internal stores through the IP_3 receptor in the ER (De, 2011; Sheldahl et al., 2003; Slusarski et al., 1997). It

Journal of Cell Science (2015) 128, 888–899 doi:10.1242/jcs.155499

is interesting to note that TRPP2 has been shown to amplify Ca^{2+} signals in mouse renal epithelial cells in a Ca^{2+}-induced Ca^{2+} release mechanism necessitating interaction between the IP_3 receptor and TRPP2 (Sammels et al., 2010). We cannot rule out the possibility that such a potential amplification mechanism might be involved in the generation of Ca^{2+} transients in kidney field cells. However, we show that disruption of RA signaling results in a dramatic decrease in TRRP2 at the plasma membrane of kidney field cells. This shows that RA can regulate TRPP2 trafficking to the plasma membrane and thus might increase intracellular Ca^{2+} signaling. Previous studies showing that RA-induced differentiation of SH-SY5Y cells (Toselli et al., 1991) or of the human teratocarcinoma cell line into NT2N neurons (Gao et al., 1998) is associated with the incorporation of new Ca^{2+} channels in the plasma membrane further support this hypothesis. Data obtained previously in animal caps also point to a role of RA in the generation of Ca^{2+} transients. Treatment of animal cap explants with activin causes induction of neural, mesodermal and endodermal derivatives. However, kidney structures are not induced. When RA is added to activin, pronephros tissue differentiates (Moriya et al., 1993), and RA, but not activin, triggers the $[Ca^{2+}]_i$ increase observed during pronephric tubule formation. Using this assay, it has also been shown that the RA-dependent induction of tubules is inhibited by the Ca^{2+} chelator BAPTA-AM, or by lanthanum, an inhibitor of TRP channels. Conversely, experimentally increasing $[Ca^{2+}]_i$ with caffeine, ionomycin or NH_4Cl can substitute to some extent for RA in inducing pronephric tubules. Treatment of animal caps with RA alone is sufficient to elicit an increase of $[Ca^{2+}]_i$ within 45 min. This process is abolished in the absence of protein synthesis (Leclerc et al., 2008).

Conclusion

We show that *pkd2* knockdown in the kidney field specifically affects *pax8* expression but not *lhx1*, *osr1* and *osr2*. It is therefore likely that *lhx1* or *osr1*, *osr2* and *pax8* are differently regulated by the signals potentially responsible for kidney field specification during gastrulation, such as RA (Cartry et al., 2006) and Wnt11b (Tételin and Jones, 2010). As outlined above, some of these genes are directly regulated by specification signals. The mechanism by which a TRPP2-dependent Ca^{2+} signaling controls *pax8* expression in the kidney field during *Xenopus* gastrulation is presented in Fig. 7 as a working model supported by our data showing that disruption of RA signals both results in an inhibition of intracellular calcium signaling (Fig. 5) and TRPP2 incorporation in the plasma membrane of kidney field cells (Fig. 6).

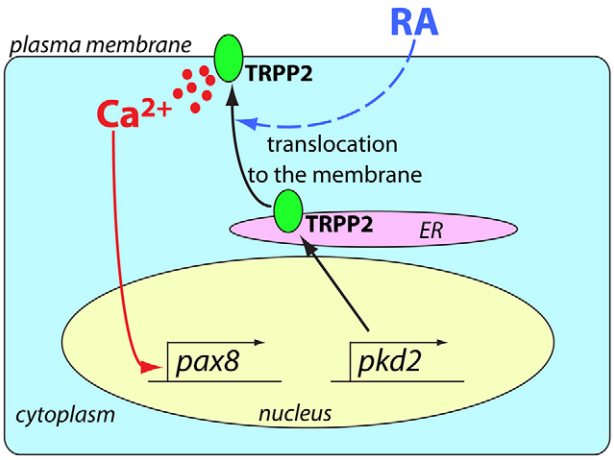

Fig. 7. A working model illustrating the mechanism by which TRPP2-dependent Ca^{2+} signaling controls *pax8* expression in the kidney field. Model is based on present data and previously published results (Cartry et al., 2006; Leclerc et al., 2008). The present work shows that *pax8* expression requires an increase in intracellular Ca^{2+} concentration $[Ca^{2+}]_i$. This increase in $[Ca^{2+}]_i$ might be due to the incorporation of TRPP2 channel, possibly under the control of RA signaling. We propose that RA is able to induce a $[Ca^{2+}]_i$ in the kidney field, as it does in embryo explants (Leclerc et al., 2008), and then indirectly controls *pax8* expression. The mechanism by which Ca^{2+} regulates *pax8* transcription is still unknown.

MATERIALS AND METHODS

Embryos manipulations

Adult *Xenopus laevis* (Daudin) were obtained from the CNRS *Xenopus* breeding Center (Rennes, France). Embryos were obtained, raised and staged using standard procedures (Nieuwkoop and Faber, 1975; Sive et al., 2000). All animal experiments were performed according to approved guidelines.

Constructs

Cloning of *pkd2* cDNA was performed from NF stage 35–36 cDNA pools. A 599-nucleotide (nt) fragment was amplified by PCR using primers corresponding to conserved regions (forward, 5′-AGGTT-ATTGGTTGAATTCCC-3′; reverse 5′-CGGAATTGGGTGAAGATA-CA-3′). This sequence was expanded by 5′ and 3′ RACE PCR using the SMARTer™ RACE cDNA amplification kit (Clontech). A 2953-nt cDNA containing the full coding sequence (accession number HG421008) was obtained by end-to-end PCR. It encodes a 947-amino-acid protein with 67.7% identity with human TRPP2 (supplementary material Fig. S1). PCR mutagenesis was performed to introduce silent mutations downstream of the start AUG in order to avoid binding to Pkd2-MO in rescue experiments (5′-AUGAAUCCCAGCAGAAUCAAA-3′ to 5′-AUGAA**C**CC**GUCAC**G**U**AUCAA**G**-3′). The mutated fragment was subcloned into pSP64TBX for synthesis of functional mRNA. Coding sequences of GFP–aequorin (Baubet et al., 2000) and human TRPP2 with GFP inserted after amino acid 157 (Hoffmeister et al., 2011) were both subcloned into pCS2+.

mRNA and morpholino microinjection

Synthesis of capped mRNA was performed as previously described (Umbhauer et al., 2000). Plasmids linearization was performed as follows: pSP64TBX-mutpkd2 with *Sal*I, pCS2+ memGFP (Moriyoshi et al., 1996) and pCS2+ GFP-aequorin with *Not*I, SP6nucβGal encoding LacZ (Smith and Harland, 1991) and PCS2+ arl13b-cherry (Borovina et al., 2010) with *Xho*I, pβSRN3-GFP with *Sfi*I (ZernickaGoetz et al., 1996), pCS2XCyp26 (Hollemann et al., 1998) with *Eco*RI, and pCS2+GFP-hPKD2 with Asp718. All plasmids were transcribed with SP6 RNA polymerase. Pkd2-MO (Tran et al., 2010) and the standard control MO (CMO) were purchased from Gene Tools. Microinjections were performed at the two- to eight-cell stage as described previously (Colas et al., 2008). Morpholino and mRNA doses are given in the results section.

In situ hybridization and LacZ staining

Whole-mount *in situ* hybridization for *pax8* (Carroll and Vize, 1999), *myod* (Hopwood et al., 1989) and *mlc* (Thézé et al., 1995), as well as staining for LacZ, were carried out as previously reported (Colas et al., 2008).

Western blotting

Embryo protein extraction was performed as previously reported (Le Bouffant et al., 2012). Immunoblotting with anti-α-tubulin has been previously described (Le Bouffant et al., 2012). Anti-polyclonal anti-human TRPP2 (Novus Biochemicals #NB100-92215), was used at 1:1000. This antibody was produced against a peptide corresponding to a

highly conserved region of the C-terminal tail of the protein (supplementary material Fig. S1). Cross-reactivity with *Xenopus* TRPP2 was controlled by western blotting. A major band of 110 kDa was detected on embryo extracts in accordance with human TRPP2 data (Giamarchi et al., 2010), together with two much fainter bands of lower mobility. Overexpression of *Xenopus* TRPP2 caused by *pkd2* mRNA injection resulted in a strong increase of this 110 kDa component, showing that it corresponds to *Xenopus* TRPP2 (supplementary material Fig. S1).

Explants dissection and immunofluorescence

For intracellular Ca^{2+} measurements and RT-QPCR analyses, archenteron wall explants corresponding to the pronephric *pax8* expression domain were dissected at late gastrula stage (NF stage 12.5–13). They were cultured in 1× modified Barth's solution (MBS).

Ionomycin- and DMSO-soaked AG1-X2 beads (BioRad) were prepared as described previously (Papanayotou et al., 2013). They were implanted at late gastrula stage (NF st.12.5) beneath the ectodermal layer overlying the kidney field. Embryos were placed in 1× MBS. A small slit was cut into epidermis with platinum wire and loop. The bead was inserted into the slit and pushed laterally with fine forceps. Implanted embryos were immediately transferred into 0.1×MMS where they were further cultured.

For immunofluorescence staining, only mesodermal and ectodermal layers were dissected. GRP explants were dissected as previously described (Schweickert et al., 2007). In all cases, explants were immediately transferred into fixative-containing Petri dishes. For anti-TRPP2 staining, explants were fixed in formaldehyde-glutaraldehyde (FG) fixative and processed for immunofluorescence staining as described (Nandadasa et al., 2009). Rabbit anti-TRPP2 antibody and mouse anti-GFP antibody (Roche) were used at 1:100 and 1:1000, respectively. Alexa-Fluor-568-conjugated anti-rabbit and Alexa-Fluor-488-conjugated anti-mouse IgG antibodies (InVitrogen) were both used at 1:1000. After washing, explants were dehydrated and cleared in benzyl benzoate in benzyl alcohol (2:1) (Dent et al., 1989) prior to confocal microscopy analysis. Monoclonal anti-acetylated tubulin staining (Sigma clone 6-11B-1, 1:500) of primary cilia was carried out as described previously (Stubbs et al., 2008), except that Alexa-Fluor-488-conjugated anti-mouse IgG antibodies were used. mCherry–arl13b-expressing explants were fixed as for anti-acetylated tubulin staining, washed and processed for confocal microscopy. Observations were carried out on Leica SPE and SP5 inverted confocal microscopes. Whole-mount immunofluorescence for 3G8 antibody was carried out as described previously (Vize et al., 1995) with Alexa-Fluor-568-conjugated anti-mouse IgG antibodies (InVitrogen) (1:1000).

Lateral marginal zone explants from embryos injected with GFP or a mix of GFP and Cyp26 mRNA were dissected at early gastrula stage and cultured until early neurula stage for RT-QPCR analysis as previously described (Le Bouffant et al., 2012).

Real-time quantitative PCR

The protocol for RT-QPCR analysis of gene expression, has been described previously (Le Bouffant et al., 2012). Primer sequences are given in supplementary material Table S3.

Microinjection and flash photolysis of caged-compounds

Injection was performed into the lateral marginal zone of four-cell stage embryos. 10 nl of Diazo-2 (Diazo-2 tetrapotassium salt is a cell impermeant caged BAPTA; 50 mM dissolved in distilled water, Molecular Probes) was co-injected with lacZ-encoding RNA (250–500 pg) as a lineage tracers. UV photolysis was performed as described previously (Leclerc et al., 2008).

Ca^{2+} measurements, temporal data acquisition and analysis

Intracellular Ca^{2+} measurements were performed with the bioluminescent Ca^{2+} probe GFP–aequorin (the GFP–aequorin construct is a gift from Jean-René Martin, CNRS, Gif-sur-Yvette, France). 10 nl of a mixture of GFP–aequorin mRNA (200 pg) and either Pkd2-MO or CMO was injected into the left V2 blastomere. Kidney field explants corresponding to the pronephric *pax8*-expression domain were dissected at the late gastrula stage (NF stage 12.5–13). Functional aequorin was reconstituted by incubating the kidney field explants with 1 ng/ml of cp-coelenterazine (Molecular Probes; stock prepared in ethanol). The kidney field explants were then processed for bioluminescence photon counting using a PMT as described previously (Leclerc et al., 2000). The activity of aequorin *in vivo* is not modified by fusion with EGFP (Baubet et al., 2000). Background noise is less than 5 photons/s. Data were collected every 1 s over a period of at least 4 h. Burn-out experiments using Triton X-100 to lyse the explant showed that when signals were not observed aequorin was not a limiting factor. Data are expressed in relative arbitrary units, proportional to the photon number. Data were selected for detailed analysis according to the following criteria: (1) explants did not dissociate during the course of the experiment; (2) intact control embryos developed normally.

TIRF microscopy

Kidney field explants expressing hTRPP2–GFP were dissected at the end of gastrulation (NF stage 12.5–13) and immediately fixed in 4% paraformaldehyde. For the observations, kidney field explants were mounted in PBS. GFP was imaged using a Nikon Eclipse TIRF microscope with a 60× objective oil immersion NA 1.49 (Fig. 6A). Excitation was performed at 488 nm and the emitted fluorescence was recorded with an Andor iXON EMCCD camera. TIRF penetration depth was set to 120 nm. Observations were performed on mesoderm. Background-subtracted fluorescent pixels were processed with a custom-made analysis routine written for Image J. The area of expression of TRPP2 channels labelled with GFP was calculated for 10 to 20 fields of 50×50 µm on four different explants overexpressing either hTRPP2–GFP mRNA alone or hTRPP2–GFP mRNA in presence of Cyp26 mRNA at 350 pg or 700 pg (Hoffmeister et al., 2011).

Acknowledgements

We thank S. Authier and E. Manzoni for excellent technical assistance in the maintenance of the *Xenopus* animal facility. We also want to thank C. Vesque for invaluable advice and criticisms concerning primary cilia experiments, Brian Ciruna for the mCherry–arl13b construct, J. R. Martin for the GFP–aequorin construct, R. Witzgall for the GFP–human TRPP2 construct, and E. Jones for the 3G8 antibody. We are very grateful to S. Bolte, R. Schwartzmann and J. F. Gilles for confocal imaging (core facility cell imaging, IFR83 CNRS, UPMC). C.L., I.N. and M.M. are members of the GDRE 731 ''Ca^{2+} toolkit proteins as drug targets in animal and plant cells''.

Competing interests

The authors declare no competing or financial interests.

Author contributions

M.F. was responsible for design, execution and interpretation of experiments, and preparation of the article; C.L. was responsible for conception, design, execution and interpretation of experiments, and preparation of the article; R.L.B. was responsible for execution and interpretation of experiments; I.B. was responsible for execution of the experiments; I.N. was responsible for execution of the experiments; M.U. was responsible for execution of the experiments; M.M. was responsible for conception, design, execution and interpretation of the experiments and preparation of the article; J.F.R. was responsible for conception, design, execution and interpretation of the experiments and preparation of the article.

Funding

This work was supported by grants from CNRS and from Université Pierre et Marie Curie (UPMC). We acknowledge funding from Émergence-UPMC-2009 research program. M.F. is financed by a 2010–2013 contract doctoral from the 'Complexité du Vivant' doctoral school.

Supplementary material

Supplementary material available online at
http://jcs.biologists.org/lookup/suppl/doi:10.1242/jcs.155499/-/DC1

References

Adams, S. R., Kao, J. P. Y. and Tsien, R. Y. (1989). Biologically useful chelators that take up calcium upon illumination. *J. Am. Chem. Soc.* **111**, 7957-7968.

Axelrod, D. (2008). Chapter 7: Total internal reflection fluorescence microscopy. *Methods Cell Biol.* **89**, 169-221.
Baubet, V., Le Mouellic, H., Campbell, A. K., Lucas-Meunier, E., Fossier, P. and Brûlet, P. (2000). Chimeric green fluorescent protein-aequorin as bioluminescent Ca2+ reporters at the single-cell level. *Proc. Natl. Acad. Sci. USA* **97**, 7260-7265.
Bisgrove, B. W., Snarr, B. S., Emrazian, A. and Yost, H. J. (2005). Polaris and Polycystin-2 in dorsal forerunner cells and Kupffer's vesicle are required for specification of the zebrafish left-right axis. *Dev. Biol.* **287**, 274-288.
Borovina, A., Superina, S., Voskas, D. and Ciruna, B. (2010). Vangl2 directs the posterior tilting and asymmetric localization of motile primary cilia. *Nat. Cell Biol.* **12**, 407-412.
Bracken, C. M., Mizeracka, K. and McLaughlin, K. A. (2008). Patterning the embryonic kidney: BMP signaling mediates the differentiation of the pronephric tubules and duct in Xenopus laevis. *Dev. Dyn.* **237**, 132-144.
Brennan, H. C., Nijjar, S. and Jones, E. A. (1998). The specification of the pronephric tubules and duct in Xenopus laevis. *Mech. Dev.* **75**, 127-137.
Brennan, H. C., Nijjar, S. and Jones, E. A. (1999). The specification and growth factor inducibility of the pronephric glomus in Xenopus laevis. *Development* **126**, 5847-5856.
Carroll, T. J. and Vize, P. D. (1999). Synergism between Pax-8 and lim-1 in embryonic kidney development. *Dev. Biol.* **214**, 46-59.
Cartry, J., Nichane, M., Ribes, V., Colas, A., Riou, J. F., Pieler, T., Dollé, P., Bellefroid, E. J. and Umbhauer, M. (2006). Retinoic acid signalling is required for specification of pronephric cell fate. *Dev. Biol.* **299**, 35-51.
Caspary, T., Larkins, C. E. and Anderson, K. V. (2007). The graded response to Sonic Hedgehog depends on cilia architecture. *Dev. Cell* **12**, 767-778.
Chan, T. C., Takahashi, S. and Asashima, M. (2000). A role for Xlim-1 in pronephros development in Xenopus laevis. *Dev. Biol.* **228**, 256-269.
Chung, M. I., Peyrot, S. M., LeBoeuf, S., Park, T. J., McGary, K. L., Marcotte, E. M. and Wallingford, J. B. (2012). RFX2 is broadly required for ciliogenesis during vertebrate development. *Dev. Biol.* **363**, 155-165.
Clapham, D. E., Julius, D., Montell, C. and Schultz, G. (2005). International Union of Pharmacology. XLIX. Nomenclature and structure-function relationships of transient receptor potential channels. *Pharmacol. Rev.* **57**, 427-450.
Colas, A., Cartry, J., Buisson, I., Umbhauer, M., Smith, J. C. and Riou, J. F. (2008). Mix.1/2-dependent control of FGF availability during gastrulation is essential for pronephros development in Xenopus. *Dev. Biol.* **320**, 351-365.
D'Andrea, B., Di Palma, T., Mascia, A., Motti, M. L., Viglietto, G., Nitsch, L. and Zannini, M. (2005). The transcriptional repressor DREAM is involved in thyroid gene expression. *Exp. Cell Res.* **305**, 166-178.
De, A. (2011). Wnt/Ca2+ signaling pathway: a brief overview. *Acta Biochim. Biophys. Sin. (Shanghai)* **43**, 745-756.
Dent, J. A., Polson, A. G. and Klymkowsky, M. W. (1989). A whole-mount immunocytochemical analysis of the expression of the intermediate filament protein vimentin in Xenopus. *Development* **105**, 61-74.
Dressler, G. R. (2009). Advances in early kidney specification, development and patterning. *Development* **136**, 3863-3874.
Gao, Z. Y., Xu, G., Stwora-Wojczyk, M. M., Matschinsky, F. M., Lee, V. M. and Wolf, B. A. (1998). Retinoic acid induction of calcium channel expression in human NT2N neurons. *Biochem. Biophys. Res. Commun.* **247**, 407-413.
Giamarchi, A., Feng, S., Rodat-Despoix, L., Xu, Y., Bubenshchikova, E., Newby, L. J., Hao, J., Gaudioso, C., Crest, M., Lupas, A. N. et al. (2010). A polycystin-2 (TRPP2) dimerization domain essential for the function of heteromeric polycystin complexes. *EMBO J.* **29**, 1176-1191.
Hoffmeister, H., Babinger, K., Gürster, S., Cedzich, A., Meese, C., Schadendorf, K., Osten, L., de Vries, U., Rascle, A. and Witzgall, R. (2011). Polycystin-2 takes different routes to the somatic and ciliary plasma membrane. *J. Cell Biol.* **192**, 631-645.
Hollemann, T., Chen, Y., Grunz, H. and Pieler, T. (1998). Regionalized metabolic activity establishes boundaries of retinoic acid signalling. *EMBO J.* **17**, 7361-7372.
Hopwood, N. D., Pluck, A. and Gurdon, J. B. (1989). MyoD expression in the forming somites is an early response to mesoderm induction in Xenopus embryos. *EMBO J.* **8**, 3409-3417.
Jones, E. A. (2005). Xenopus: a prince among models for pronephric kidney development. *J. Am. Soc. Nephrol.* **16**, 313-321.
Köttgen, M. (2007). TRPP2 and autosomal dominant polycystic kidney disease. *Biochim. Biophys. Acta* **1772**, 836-850.
Koulen, P., Cai, Y., Geng, L., Maeda, Y., Nishimura, S., Witzgall, R., Ehrlich, B. E. and Somlo, S. (2002). Polycystin-2 is an intracellular calcium release channel. *Nat. Cell Biol.* **4**, 191-197.
Le Bouffant, R., Wang, J. H., Futel, M., Buisson, I., Umbhauer, M. and Riou, J. F. (2012). Retinoic acid-dependent control of MAP kinase phosphatase-3 is necessary for early kidney development in Xenopus. *Biol. Cell* **104**, 516-532.
Leclerc, C., Webb, S. E., Daguzan, C., Moreau, M. and Miller, A. L. (2000). Imaging patterns of calcium transients during neural induction in Xenopus laevis embryos. *J. Cell Sci.* **113**, 3519-3529.
Leclerc, C., Webb, S. E., Miller, A. L. and Moreau, M. (2008). An increase in intracellular Ca2+ is involved in pronephric tubule differentiation in the amphibian Xenopus laevis. *Dev. Biol.* **321**, 357-367.
Ma, R., Li, W. P., Rundle, D., Kong, J., Akbarali, H. I. and Tsiokas, L. (2005). PKD2 functions as an epidermal growth factor-activated plasma membrane channel. *Mol. Cell. Biol.* **25**, 8285-8298.
Majumdar, A., Lun, K., Brand, M. and Drummond, I. A. (2000). Zebrafish no isthmus reveals a role for pax2.1 in tubule differentiation and patterning events in the pronephric primordia. *Development* **127**, 2089-2098.
McGrath, J., Somlo, S., Makova, S., Tian, X. and Brueckner, M. (2003). Two populations of node monocilia initiate left-right asymmetry in the mouse. *Cell* **114**, 61-73.
Mochizuki, T., Wu, G., Hayashi, T., Xenophontos, S. L., Veldhuisen, B., Saris, J. J., Reynolds, D. M., Cai, Y., Gabow, P. A., Pierides, A. et al. (1996). PKD2, a gene for polycystic kidney disease that encodes an integral membrane protein. *Science* **272**, 1339-1342.
Moriya, N., Uchiyama, H. and Asashima, M. (1993). Induction of pronephric tubules by activin and retinoic acid in presumptive ectoderm of Xenopus laevis. *Dev. Growth Differ.* **35**, 123-128.
Moriyoshi, K., Richards, L. J., Akazawa, C., O'Leary, D. D. and Nakanishi, S. (1996). Labeling neural cells using adenoviral gene transfer of membrane-targeted GFP. *Neuron* **16**, 255-260.
Nandadasa, S., Tao, Q., Menon, N. R., Heasman, J. and Wylie, C. (2009). N- and E-cadherins in Xenopus are specifically required in the neural and non-neural ectoderm, respectively, for F-actin assembly and morphogenetic movements. *Development* **136**, 1327-1338.
Nauli, S. M., Alenghat, F. J., Luo, Y., Williams, E., Vassilev, P., Li, X., Elia, A. E. H., Lu, W., Brown, E. M., Quinn, S. J. et al. (2003). Polycystins 1 and 2 mediate mechanosensation in the primary cilium of kidney cells. *Nat. Genet.* **33**, 129-137.
Nieuwkoop, P. D. and Faber, J. (1975). *Normal Table of Xenopus Laevis (Daudin): a Systematical and Chronological Survey of the Development From the Fertilized Egg till the End of Metamorphosis*. Amsterdam: North-Holland Publishing Company.
Obara, T., Mangos, S., Liu, Y., Zhao, J., Wiessner, S., Kramer-Zucker, A. G., Olale, F., Schier, A. F. and Drummond, I. A. (2006). Polycystin-2 immunolocalization and function in zebrafish. *J. Am. Soc. Nephrol.* **17**, 2706-2718.
Papanayotou, C., De Almeida, I., Liao, P., Oliveira, N. M. M., Lu, S. Q., Kougioumtzidou, E., Zhu, L., Shaw, A., Sheng, G., Streit, A. et al. (2013). Calfacilitin is a calcium channel modulator essential for initiation of neural plate development. *Nat. Commun.* **4**, 1837.
Pazour, G. J., San Agustin, J. T., Follit, J. A., Rosenbaum, J. L. and Witman, G. B. (2002). Polycystin-2 localizes to kidney cilia and the ciliary level is elevated in orpk mice with polycystic kidney disease. *Curr. Biol.* **12**, R378-R380.
Sammels, E., Devogelaere, B., Mekahli, D., Bultynck, G., Missiaen, L., Parys, J. B., Cai, Y., Somlo, S. and De Smedt, H. (2010). Polycystin-2 activation by inositol 1,4,5-trisphosphate-induced Ca2+ release requires its direct association with the inositol 1,4,5-trisphosphate receptor in a signaling microdomain. *J. Biol. Chem.* **285**, 18794-18805.
Saxen, L. (1987). *Organogenesis of the Kidney*. Cambridge: Cambridge University Press.
Schottenfeld, J., Sullivan-Brown, J. and Burdine, R. D. (2007). Zebrafish curly up encodes a Pkd2 ortholog that restricts left-side-specific expression of southpaw. *Development* **134**, 1605-1615.
Schweickert, A., Weber, T., Beyer, T., Vick, P., Bogusch, S., Feistel, K. and Blum, M. (2007). Cilia-driven leftward flow determines laterality in Xenopus. *Curr. Biol.* **17**, 60-66.
Seufert, D. W., Brennan, H. C., DeGuire, J., Jones, E. A. and Vize, P. D. (1999). Developmental basis of pronephric defects in Xenopus body plan phenotypes. *Dev. Biol.* **215**, 233-242.
Sheldahl, L. C., Slusarski, D. C., Pandur, P., Miller, J. R., Kühl, M. and Moon, R. T. (2003). Dishevelled activates Ca2+ flux, PKC, and CamKII in vertebrate embryos. *J. Cell Biol.* **161**, 769-777.
Shimomura, O. (1991). Preparation and handling of aequorin solutions for the measurement of cellular Ca2+. *Cell Calcium* **12**, 635-643.
Sive, H., Grainger, R. and Harland, R. (2000). *Early Development of Xenopus Laevis: A Laboratory Manual*. Plainview, NY: Cold Spring Harbor Laboratory Press.
Slusarski, D. C., Corces, V. G. and Moon, R. T. (1997). Interaction of Wnt and a Frizzled homologue triggers G-protein-linked phosphatidylinositol signalling. *Nature* **390**, 410-413.
Smith, W. C. and Harland, R. M. (1991). Injected Xwnt-8 RNA acts early in Xenopus embryos to promote formation of a vegetal dorsalizing center. *Cell* **67**, 753-765.
Stubbs, J. L., Oishi, I., Izpisúa Belmonte, J. C. and Kintner, C. (2008). The forkhead protein Foxj1 specifies node-like cilia in Xenopus and zebrafish embryos. *Nat. Genet.* **40**, 1454-1460.
Sun, Z., Amsterdam, A., Pazour, G. J., Cole, D. G., Miller, M. S. and Hopkins, N. (2004). A genetic screen in zebrafish identifies cilia genes as a principal cause of cystic kidney. *Development* **131**, 4085-4093.
Tena, J. J., Neto, A., de la Calle-Mustienes, E., Bras-Pereira, C., Casares, F. and Gómez-Skarmeta, J. L. (2007). Odd-skipped genes encode repressors that control kidney development. *Dev. Biol.* **301**, 518-531.
Tételin, S. and Jones, E. A. (2010). Xenopus Wnt11b is identified as a potential pronephric inducer. *Dev. Dyn.* **239**, 148-159.
Thézé, N., Hardy, S., Wilson, R., Allo, M. R., Mohun, T. and Thiebaud, P. (1995). The MLC1f/3f gene is an early marker of somitic muscle differentiation in Xenopus laevis embryo. *Dev. Biol.* **171**, 352-362.
Toselli, M., Masetto, S., Rossi, P. and Taglietti, V. (1991). Characterization of a voltage-dependent calcium current in the human neuroblastoma cell line SH-SY5Y during differentiation. *Eur. J. Neurosci.* **3**, 514-522.

Journal of Cell Science

Tran, U., Zakin, L., Schweickert, A., Agrawal, R., Döger, R., Blum, M., De Robertis, E. M. and Wessely, O. (2010). The RNA-binding protein bicaudal C regulates polycystin 2 in the kidney by antagonizing miR-17 activity. *Development* **137**, 1107-1116.

Umbhauer, M., Penzo-Méndez, A., Clavilier, L., Boucaut, J. and Riou, J. (2000). Signaling specificities of fibroblast growth factor receptors in early Xenopus embryo. *J. Cell Sci.* **113**, 2865-2875.

Vize, P. D., Jones, E. A. and Pfister, R. (1995). Development of the Xenopus pronephric system. *Dev. Biol.* **171**, 531-540.

Vize, P. D., Woolf, A. S. and Bard, J. B. L. (2003). *The Kidney: From Normal Development to Congenital Disease*. Amsterdam: Elsevier Science.

Webb, S. E. and Miller, A. L. (2006). Ca2+ signaling and early embryonic patterning during the blastula and gastrula periods of zebrafish and Xenopus development. *Biochim. Biophys. Acta* **1763**, 1192-1208.

Wingert, R. A., Selleck, R., Yu, J., Song, H. D., Chen, Z., Song, A., Zhou, Y., Thisse, B., Thisse, C., McMahon, A. P. et al. (2007). The cdx genes and retinoic acid control the positioning and segmentation of the zebrafish pronephros. *PLoS Genet.* **3**, e189.

Wu, G., Markowitz, G. S., Li, L., D'Agati, V. D., Factor, S. M., Geng, L., Tibara, S., Tuchman, J., Cai, Y., Park, J. H. et al. (2000). Cardiac defects and renal failure in mice with targeted mutations in Pkd2. *Nat. Genet.* **24**, 75-78.

Yoder, B. K., Hou, X. and Guay-Woodford, L. M. (2002). The polycystic kidney disease proteins, polycystin-1, polycystin-2, polaris, and cystin, are co-localized in renal cilia. *J. Am. Soc. Nephrol.* **13**, 2508-2516.

Zernicka-Goetz, M., Pines, J., Ryan, K., Siemering, K. R., Haseloff, J., Evans, M. J. and Gurdon, J. B. (1996). An indelible lineage marker for Xenopus using a mutated green fluorescent protein. *Development* **122**, 3719-3724.